

# Low-attenuation Large- $A_{\text{eff}}$ Optical Fiber for Long-Haul Transmission

Katsubumi Nagasu,<sup>1</sup> Kenji Yamashiro,<sup>1</sup> and Shoichiro Matsuo<sup>1</sup>

*Digital coherent technology, which enables large-capacity transmission, has been put to practical use especially in long-haul systems. Accordingly, G.654.E category <sup>1)</sup> is recommended by ITU-T as an optical fiber that can improve the optical signal-to-noise ratio (OSNR) required for systems using digital coherent technology. We have developed FutureGuide<sup>®</sup>-HSC-110 (hereafter HSC-110) and FutureGuide<sup>®</sup>-HSC-125 (hereafter HSC-125) compliant with ITU-T G.654.E. Both products have low attenuation and large  $A_{\text{eff}}$ . HSC-110 can be used in a cable with high density while HSC-125 has a high figure of merit (FOM). Both optical fibers suffer low macro- and micro-bending losses, so they can be used in cables with various structures.*

## 1. Introduction

Digital coherent technology, which enables long-haul, large-capacity transmission, has been spreading with the rapid increase in data traffic in recent years. This technology dramatically improves optical transmission performance by incorporating ultra-high-speed digital signal processing into optical fiber communication systems. The high bit-rate systems based on this technology need a high optical signal-to-noise ratio (OSNR) and low non-linear distortion. Therefore, the optical fibers require low attenuation and large effective core area ( $A_{\text{eff}}$ ). G.654.E category was recommended by ITU-T in 2016 as a suitable optical fiber for over 100 Gbit/s digital coherent terrestrial networks.

On the other hand, higher-density optical cables have come to widespread use to build optical fiber communication networks more economically and efficiently, with increasing capacity by digital coherent technology. The demand for higher density optical cables is expected to increase for ITU-T G.654.E-compliant optical fibers as well.

We have developed FutureGuide<sup>®</sup>-HSC-110 (HSC-110) and FutureGuide<sup>®</sup>-HSC-125 (HSC-125) as the optical fiber compliant with ITU-T G.654.E. HSC-110 is suitable for high-density cables for its low bending loss while HSC-125 is focused on improving OSNR by taking advantage of its large  $A_{\text{eff}}$ . In addition, both optical fibers have been designed to prevent the degradation of macro- and micro-bending properties caused by enlargement of the  $A_{\text{eff}}$  and to allow the use of ring-marks for easy identification of optical fibers. Thus, the optical fibers are suitable for large-fiber-count cables expected to be used in the trunk networks.

## 2. The properties required for optical fibers for long-haul transmission

An optical signal is attenuated as it propagates downward, from a transmitter to a receiver. If the received signal power is smaller than the detection limit of the receiver, the original signal cannot be recovered from the detected signal anymore. Therefore, it is important to prevent a decrease in an OSNR, which is the ratio of optical signal to noise, for long-haul transmission. Multilevel modulation systems using digital coherent technologies require a higher OSNR than conventional intensity modulation systems.

There are two ways to improve an OSNR: by increasing optical signal power at a transmitter, and by reducing the attenuation of optical signal power. When optical signal power is increased, signal waveform distortion due to non-linear effects (non-linear distortion) in an optical fiber becomes a problem. The non-linear distortion originates from the Kerr effect, which is a refractive index change according to optical intensity, and it is expressed in (Eq. 1).

$$n = n_0 + n_2 \frac{P}{A_{\text{eff}}} \quad (\text{Eq. 1})$$

Where  $n$  is the refractive index,  $n_0$  is the linear refractive index,  $n_2$  is the non-linear refractive index,  $P$  is the optical signal power. Equation 1 shows that there are two ways to reduce the non-linear distortion: by decreasing the non-linear refractive index of the optical fiber, and by reducing the density of optical signal power by enlarging the  $A_{\text{eff}}$ . Another OSNR improvement method, reducing attenuation of the optical fiber, is effective in preventing the attenuation of optical signal power.

Figure of merit (FOM) is used as a metric to determine the OSNR improvement based on the properties of

---

<sup>1</sup> Optical Fiber Development Department Optical Fiber Division

**Panel 1. Abbreviations, Acronyms, and Terms.**

ITU-T—International Telecommunication Union  
Telecommunication Standardization Sector  
OSNR—Optical signal to noise ratio  
 $A_{\text{eff}}$ —Effective core area  
Effective optical signal transmitting area in an optical fiber  
FOM—Figure of merit  
IEC—International Electrotechnical Commission  
O-band—Original-band  
One of the optical communication wavelength bands. The wavelength band is from 1260 to 1360 nm.  
C-band—Conventional-band  
One of the optical communication wavelength bands. The wavelength band is from 1530 to 1565 nm.

L-band —Long-wavelength-band  
One of the optical communication wavelength bands. The wavelength band is from 1565 to 1625 nm.  
Fusion splicing of optical fibers—Splicing methods that melt end faces of optical fibers by high-voltage arc discharge and splice them together after aligning each axis of the end faces.  
MFD—Mode field diameter  
Diameter of the optical signal power distribution area in an optical fiber

an optical fiber and is defined by Eq. 2<sup>2)</sup>.

$$FOM \text{ (dB)} = 10 \log \left( \frac{A_{\text{eff}}}{n_2} \cdot \frac{n_{2\text{-ref}}}{A_{\text{eff-ref}}} \right) - (\alpha - \alpha_{\text{ref}}) \cdot L - 10 \log \left( \frac{L_{\text{eff}}}{L_{\text{eff-ref}}} \right) \quad (\text{Eq. 2})$$

Where  $\alpha$  is the attenuation (dB/km),  $L$  is the span length (repeater interval, km),  $L_{\text{eff}}$  is the effective length (km) defined by Eq. 3.

$$L_{\text{eff}} = \frac{1 - \exp(-\alpha L)}{\alpha} \quad (\text{Eq. 3})$$

The parameters with the suffix “ref” denote those of a reference fiber. Equation 2 also shows that a low non-linear refractive index, a large  $A_{\text{eff}}$ , and a low attenuation contribute to the improvement of an OSNR.

The non-linear refractive index of glass depends on the concentration of dopants. For example, the non-linear refractive index of silica glass increases with increasing concentration of Germanium (Ge)<sup>3)</sup>. Therefore, the non-linear refractive index of a conventional optical fiber, which is doped with Ge in the core, is higher than an optical fiber with a pure silica glass core. Figure 1 shows the index profile of the Ge-doped optical fiber and silica-core optical fiber. The horizontal axis shows the radius, and the vertical axis the refractive index. For the Ge-doped optical fiber, doping the core with Ge changes the refractive index from that of the cladding. By contrast, for the silica-core optical fiber, the cladding is doped with fluorine (F) to make a difference in the refractive index from that of the core. Since the nonlinear refractive index of the silica-core optical fiber is only about 96% compared to that of the conventional Ge-doped core optical fiber, the improvement of the FOM by using the silica-core optical fiber is only about 0.19 dB. This indicates that the improvement by changing the material composition of optical fibers is only marginal.

It is effective to reduce the attenuation and to enlarge the

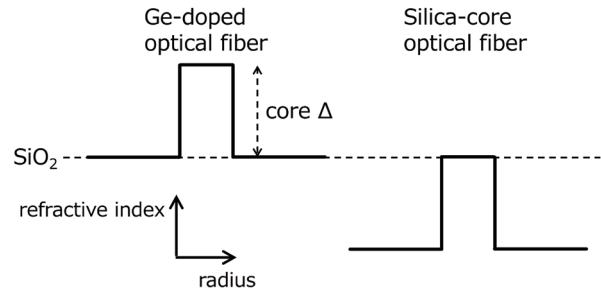


**Fig. 1. Schematic refractive index of Ge-doped optical fiber and silica-core optical fiber.**

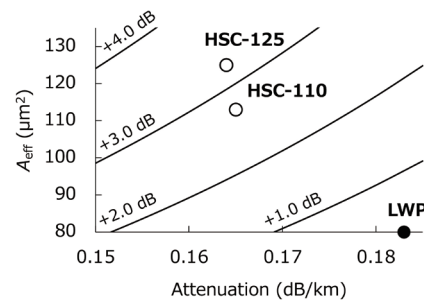


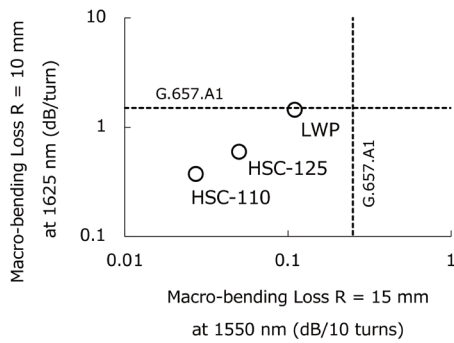
**Fig. 2. Influence of attenuation and  $A_{\text{eff}}$  on the FOM.**

$A_{\text{eff}}$  for a significant FOM improvement. Figure 2 shows the effect of an attenuation and an  $A_{\text{eff}}$  on the FOM. A conventional optical fiber, FutureGuide®-LWP (hereafter LWP) with an attenuation of 0.183 dB/km, and  $A_{\text{eff}}$  of 80  $\mu\text{m}^2$ , at 1550 nm, was used as a reference for the FOM. The span length was set at 80 km. An improvement in FOM of more than 1.0 dB can be expected by reducing the transmission loss to about 0.165 dB/km for the optical fiber with the same  $A_{\text{eff}}$  as LWP. Furthermore, for an optical fiber with an  $A_{\text{eff}}$  enlarged to over 110  $\mu\text{m}^2$ , the FOM is improved to about 3 dB.

In reducing attenuation, the silica core structure mentioned above is effective since the core does not contain any dopant such as Ge or F, which cause concentration fluctuation. This enables silica-core optical fibers to achieve lower attenuation than Ge-doped optical

**Table 1. Optical characteristics of HSC-110, HSC-125.**

	Condition	HSC-110	HSC-125	ITU-T G.654.E	LWP	Unit
Attenuation	1550 nm	0.165	0.164	$\leq 0.23$	0.183	dB/km
	1625 nm	0.180	0.180	-	0.196	dB/km
MFD	1550 nm	11.7	12.3	11.5-12.5 Tolerance $\pm 0.7$	10.5	$\mu\text{m}$
$A_{\text{eff}}$	1550 nm	113	125	-	80	$\mu\text{m}^2$
Cable cutoff wavelength	-	$\leq 1530$	$\leq 1520$	$\leq 1530$	$\leq 1260$	nm
Macro-bending loss	R = 30 mm 100 turns 1625 nm	$\leq 0.1$	$\leq 0.1$	$\leq 0.1$	$\leq 0.1$	dB
Chromatic dispersion coefficient	1550 nm	21	21	17-23	17	ps/(nm·km)
Dispersion slope	1550 nm	0.060	0.060	0.050-0.070	-	ps/(nm <sup>2</sup> ·km)

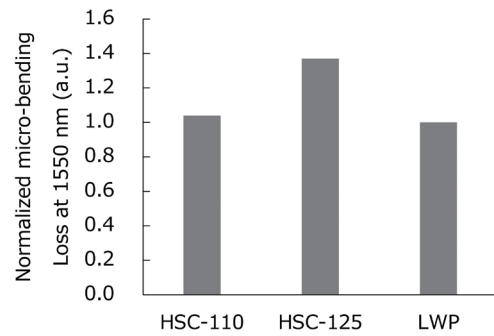
**Fig. 3. Macro-bending losses at a bending radius of 10 mm and 15 mm.**

fibers. Density fluctuation due to inhomogeneity in the glass network structure and concentration fluctuation due to dopants such as Ge and F cause Rayleigh scattering, which accounts for up to 80% of optical attenuation.

In order to enlarge an  $A_{\text{eff}}$ , it is necessary to reduce a refractive index difference between a core and a cladding and enlarge a core diameter. However, a low-delta structure leads to an increase in macro- and micro-bending losses, and therefore, a design trade-off between enlargement of  $A_{\text{eff}}$  and bend properties. Since optical fibers in a cable are subjected to lateral pressure and bending, an excessive increase in macro- and micro-bending losses with enlargement of  $A_{\text{eff}}$  must be prevented for the use of the fibers in various types of cables.

### 3. Basic properties of the newly developed products

Based on the above-mentioned properties required for an optical fiber, we have developed two types of optical fibers (HSC-110, HSC-125) for long-haul transmission in compliance with ITU-T G.654.E. Table 1 shows the main optical properties of these products. ITU-T G.654.E standards and properties of LWP are shown in the table for comparison. A typical attenuation at 1550 nm is 0.165 dB/km for HSC-110 and 0.164 dB/km for HSC-125. By adopting the silica-core structure, the attenuations are about 0.02 dB/km lower than that of LWP of the Ge-core structure. The  $A_{\text{eff}}$  at 1550 nm is 113  $\mu\text{m}^2$  for HSC-110 and

**Fig. 4. Micro-bending losses of HSC-110, HSC-125.**

125  $\mu\text{m}^2$  for HSC-125, which are from 40% to 50% larger than LWP. The improvements of the FOM were 2.7 dB for HSC-110 and 3.2 dB for HSC-125 as shown in Fig. 2. HSC-125 is superior to HSC-110 in terms of improvement in the FOM.

On the other hand, HSC-110 has superior properties than HSC-125 in terms of macro- and micro-bending losses, HSC-110 can be used in high-density cables. The features of HSC-110 and HSC-125 are described regarding a macro- and micro-bending in the following.

Bending losses can be categorized into macro-bending loss and micro-bending loss. The macro-bending loss is a power loss caused by bending an optical fiber with a bending radius of several mm to several 10 mm, and a micro-bending loss is a power loss when an optical fiber receives lateral pressure from a small uneven surface. Both of the bending losses need to be reduced to minimize attenuation in a cable.

The macro-bending losses of the new products have met the properties required by ITU-T G.654.E (bending radius 30 mm, 100 turns, below 0.1 dB loss increase at 1625 nm) as shown in the Table 1. Furthermore, the macro-bending loss of HSC-110 satisfied ITU-T G.657. A1 <sup>4)</sup>, a recommendation for a low-bending-loss optical fiber. ITU-T G.657.A1 is one of the categories in ITU-T G.657 specifying losses with a small bending radius of 15 mm or less to support optimizing the bending and handling characteristics in a limited space. Figure 3 shows macro-bending losses of HSC-110, HSC-125 and LWP with bending radi of 10 mm and 15 mm. The dotted lines are the upper limit of ITU-T G.657.A1. The new optical

fibers are less susceptible to macro-bending than LWP, and especially, HSC-110 fully has satisfied the standard of ITU-T G.657.A1. The reason the macro-bending loss of HSC-110 is smaller than HSC-125 is because HSC-110 has been designed to have a smaller  $A_{eff}$ . On the other hand, the new products suffer lower macro-bending loss even though their  $A_{eff}$  are larger than LWP because the cable cut-off wavelengths are longer than LWP. The conventional LWP requires a cut-off wavelength shorter than 1260 nm to ensure single mode transmission at the O-band or longer. On the other hand, since ITU-T G.654.E focusing on long-haul transmission is intended for single mode transmission use at the C-band or longer. Therefore, a cut-off wavelength longer than LWP is acceptable for the new optical fibers.

Figure 4 shows a comparison of micro-bending sensitivities. We measured micro-bending sensitivities of the three products by conducting the fixed diameter sandpaper drum test (SP test) specified by IEC TR 62221<sup>5)</sup> method B. Test fibers were wound onto a 400-mm-diameter drum coated with a 360-grid sandpaper and the attenuation of each product was measured. The tension on the fiber during the winding was 1.0 N. Micro-bending sensitivity tends to increase rapidly as  $A_{eff}$  enlarges. However, the new products had the same level of micro-bending performance even though their  $A_{eff}$  were enlarged to more than 40% compared with LWP. Excellent micro-bending performance was obtained by using a softer coating material than LWP.

As mentioned above, since the new products have the macro- and micro-bending losses equal or lower than the conventional LWP despite the large  $A_{eff}$ , they can be used in the cables of various structures. In particular, we reported the excellent performance of HSC-110 in a ribbon slot cable<sup>6)7)</sup>, and it is also suitable for a high-density cable for the lower macro- and micro-bending losses.

#### 4. Attenuation of ring-marked optical fiber

For cables with an extremely large number of fibers per cable, such as ultra-high-density cables, combining multiple ring-marks and colors simplifies the identification of the optical fibers. For example, as shown in the Fig. 5, the variations from no ring-mark to triple ring-marks allow the identification of 4 optical fibers. In addition, 13 different colors enable the identification of 52 optical fibers.

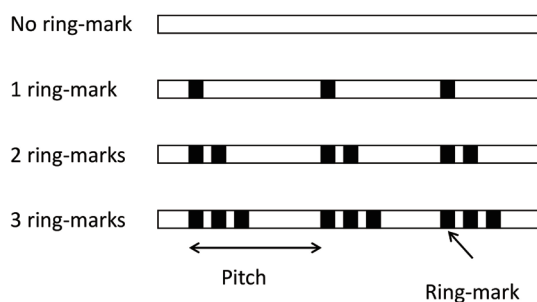


Fig. 5. Ring-mark pattern.

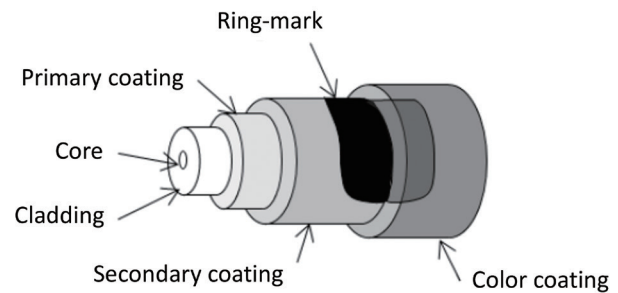


Fig. 6. Schematic of the ring-marked optical fiber.

Table 2. Relationship between ring-mark and loss increase.

Pitch	Number of marks	Loss increase @1550 nm (dB/km)
200 mm	1	0.000
200 mm	2	0.000
200 mm	3	0.001

Figure 6 shows a schematic of a ring-marked optical fiber. Since the ring-marks are a-few-micrometer-thick ink layers printed on the secondary coating layer, lateral pressure generated due to unevenness of the ring-marks is periodically applied on the optical fiber inside the cable. The ring-marked optical fibers are more prone to an increase in micro-bending loss than normal optical fibers, and an increase in attenuation by applying the ring-marks is undesirable from a practical standpoint. Table 2 shows the change in attenuation caused by applying the ring-marks to HSC-125 with a higher micro-bending loss than HSC-110. We tested for the attenuation increase of the bobbin-wound optical fibers, each of which was marked with 1 to 3 ring-marks in a 200 mm pitch. The results showed the attenuation increase was very low even for the fiber with 3 ring-marks, which is most severely affected by micro-bending loss. Figure 7 shows an attenuation spectra of 3-ring-marked optical fiber. The attenuation spectra with and without the ring-marks are almost the same in the L-band as well as in the C band. Therefore, the new products can be used in trunk networks, where each cable needs numerous ring-marked optical fibers.

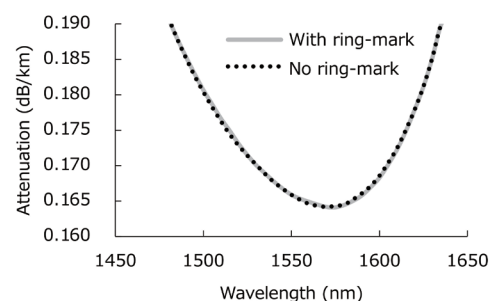


Fig. 7. Attenuation spectra of ring marked optical fiber.

#### 5. Transmission properties including splice losses

Since splices between optical cables and splices between optical cables and repeaters are repeated in long-haul transmission systems, transmission characteristics including the splice losses should be evaluated. Both of

splices of homogeneous optical fibers in cable laying and splices of heterogeneous optical fibers in repeaters should be considered. The splice losses can be estimated using (Eq. 4) <sup>8)</sup>.

$$SpliceLoss(dB) = -10 \log \left[ \left( \frac{2w_1w_2}{w_1^2 + w_2^2} \right)^2 \exp \left( \frac{-2d^2}{w_1^2 + w_2^2} \right) \right] \quad (\text{Eq. 4})$$

Where  $2w_1$  and  $2w_2$  are the MFD of optical fibers,  $d$  is the amount of axial misalignment. The splice loss, which is estimated using Eq. 4, between a conventional optical fiber and an optical fiber with a different MFD are indicated in Fig. 8 as a solid line. Since a splice loss between optical fibers with a large difference in MFD is high, a splice loss of a conventional optical fiber in the repeater is assumed to be higher than the homogeneous splice.

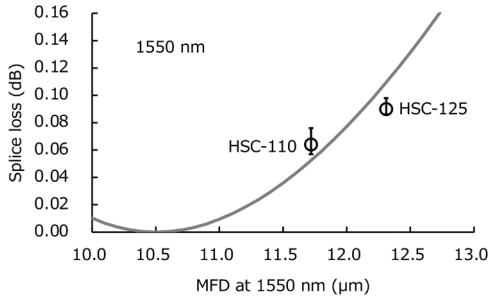


Fig. 8. Calculated splice losses as functions of MFDs and measured splice losses between conventional optical fiber and HSC-110, HSC-125.

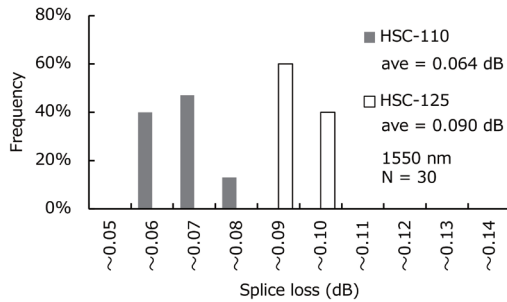


Fig. 9. Heterogeneous splice losses between conventional optical fiber and HSC-110, HSC-125.

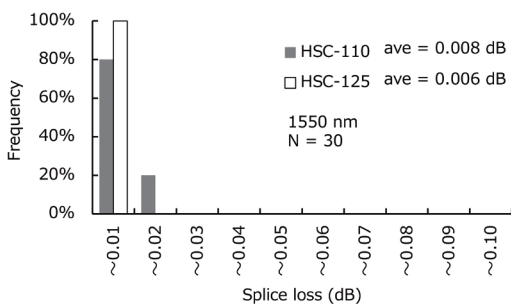


Fig. 10. Homogeneous splice losses of HSC-110, HSC-125.

Figure 9 shows the heterogeneous splice losses between

the newly developed optical fibers and a conventional optical fiber, and Fig. 10 compares the homogeneous splice losses of the optical fibers. A fusion splicer, Fujikura FSM-70S, was used. We tested 30 times with the normal SM splice conditions. The maximum splice losses at a wavelength of 1550 nm between HSC-110 and the conventional optical fiber was 0.06 dB, and between HSC-125 and the conventional optical fiber was 0.09 dB. The splice losses were almost the same as the estimated value in Fig. 8. On the other hand, the maximum values of homogeneous splice loss were all less than 0.01 dB.

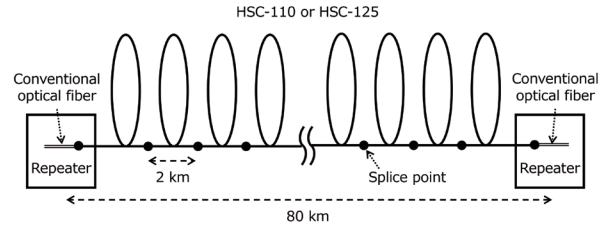


Fig. 11. Evaluation model of transmission characteristics including splice losses.

Figure 11 shows a transmission line model with a span length of 80 km. To determine the impact of the splice losses in transmission performance, we estimated the FOM using the model. We assumed splices between homogeneous optical fibers at cable splice points 2 km apart and splices with conventional optical fibers in repeaters at both ends. The total attenuation of the transmission line is calculated as the sum of attenuation in the optical fiber per a span length, splice losses between homogeneous optical fibers, and splice losses in conventional optical fibers in repeaters. The total attenuations of the transmission line were 0.176 dB/km for HSC-110 and 0.174 dB/km for HSC-125. The values were calculated using the splice losses in consideration of the combination variation of MFDs and the axial misalignment assumed in the actual transmission line. On the other hand, assuming the transmission line using the conventional optical fiber instead of HSC, the total attenuation of the transmission line was 0.192 dB/km. Using the conventional optical fiber as a reference, the improvements in FOM as the transmission line estimated using Eq. 2 were 2.7 dB for HSC-110 and 3.2 dB for HSC-125, which were equivalent to the FOM before considering splice losses. From the above results, even if the splice losses in the actual transmission line are considered, improvements in the transmission characteristics can be expected by using the new products in terms of the FOM.

## 6. Conclusion

We have developed HSC-110 and HSC-125 compliant with ITU-T G.654.E. The optical fibers have been designed to minimize macro- and micro-bending losses with increasing  $A_{\text{eff}}$  and to allow the use of ring-marks to facilitate the identification of optical fibers. Consequently, the optical fibers can be used in a cable with many fibers expected to be employed in trunk networks. In particular, HSC-110 will be introduced to our high density slot-less

cable, WTC (Wrapping Tube Cable<sup>®</sup>), because of its excellent performance, specifically, low macro- and micro-bending losses.

## References

- 1) International Telecommunications Union, "ITU-T G.654: Characteristics of a cut-off shifted single-mode optical fibre and cable," 2020.
- 2) J.D. Downie, "112 Gb/s PM-QPSK transmission systems with reach lengths enabled by optical fibers with ultra-low loss and very large effective area," Proceedings of SPIE, Vol.8284, 828403, 2012.
- 3) A. Wada, S. Okude, T. Sakai, and R. Yamauchi, "GeO<sub>2</sub> concentration dependence of nonlinear refractive index coefficients of silica-based optical fibers," Electron. Commun. Jpn. Part Commun. Vol.79, Issue.11, pp.12–19, 1996.
- 4) International Telecommunications Union, "ITU-T G.657: Characteristics of a bending-loss insensitive single-mode optical fibre and cable," 2016.
- 5) International Electrotechnical Commission, "IEC/TR 62221:Optical Fibres – Measurement methods – Microbending sensitivity," 2012.
- 6) T. Nunome, K. Nagasu, T. Shoji, K. Okada, D. Sega, R. Maruyama, I. Ishida, A. Namazue, and S. Matsuo, "Low attenuation and large  $A_{\text{eff}}$  optical fibers optimized for long-haul application," Proceedings of the 65th IWCS Conference, 10-3, Oct. 2016.
- 7) D. Sega, K. Okada, R. Maruyama, K. Nagasu, H. Nakagome, T. Onodera, A. Murata, and S. Matsuo, "Low attenuation and large  $A_{\text{eff}}$  fiber with a matched-cladding profile," Proceedings of the 66th IWCS Conference, pp.638-643, Oct. 2017.
- 8) D. Marcuse, "Loss analysis of single-mode fiber splice," Bell Syst. Tech. J., Vol.56, no.5, pp.703-718, 1977.